

# 3D printing of gradient-doped Yb: YAG laser ceramics by leveraging active mixing

Mengmeng Xie <sup>a, c</sup>, Haohao Ji <sup>b, c</sup>, Dewen Wang <sup>b, c</sup>, Junping Wang <sup>b, c</sup>, Jian Zhang <sup>b, c, \*</sup>, Yu Liu <sup>a, \*</sup>, Dianzi Liu <sup>d, \*</sup>, Shiwei Wang <sup>b, c</sup>, Nianjiang Chen <sup>e</sup>, Lei Wang <sup>f</sup>, Yuan Gao <sup>f</sup>

<sup>a</sup> School of Mechanical Engineering, Jiangnan University, Wuxi, Jiangsu, 214122, China

<sup>b</sup> Center of Materials Science and Optoelectronics Engineering, University of Chinese Academy of Sciences, Beijing, 100049, China

<sup>c</sup> State Key Laboratory of High Performance Ceramics and Superfine Microstructure, Shanghai Institute of Ceramics, Chinese Academy of Sciences, Shanghai, 200050, China

<sup>d</sup> School of Engineering, University of East Anglia, Norwich, NR4 7TJ, UK

<sup>e</sup> Science and Technology on Solid-State Laser Laboratory, Beijing, 100015, China

<sup>f</sup> Qian Xuesen Laboratory of Space Technology, China Academy of Space Technology, Beijing, 100081, China

\* Corresponding authors.

*E-mail address:* [jianzhang@mail.sic.ac.cn](mailto:jianzhang@mail.sic.ac.cn) (J. Zhang),

[yuliu@jiangnan.edu.cn](mailto:yuliu@jiangnan.edu.cn) (Y. Liu),

[Dianzi.Liu@uea.ac.uk](mailto:Dianzi.Liu@uea.ac.uk) (D. Z. Liu).

## Abstract

Gradient-doped laser ceramics by 3D printing method have great potentials for high-power laser applications. However, it is challenging for fabricating such type of gain media since different component slurries, as prepared offline, are inconvenient to be precisely fabricated by traditional methods. To address these issues, a facile approach for additive manufacturing of high-power laser ceramics has been proposed for the gradient structure fabrication. First, a material extrusion-based 3D printing device with a home-made active mixing module has been developed to fabricate gradient-doped Yb: YAG(Y<sub>3</sub>Al<sub>5</sub>O<sub>12</sub>) laser ceramics using only two slurries with different doping concentrations. Following that, the active mixing module has been systematically investigated to obtain different Yb doped concentrations of printing slurries with uniform element distribution. By measuring the switching delay volume between different components, the proper volume adjustment has enabled the Yb concentration distribution of green bodies to be consistent with the designed profile in the 3D process. Finally, multi-component (0-5-10-5-0 at. % Yb: YAG) green bodies have been printed, and experimental tests have been conducted to evaluate the performances of these gradient-

doped laser ceramics. Results have shown that the gradient-doped ceramic has obtained 82.1% in-line transmittance at 1100 nm (4.6 mm thickness, along with the doping concentration gradient) and the average Yb ions diffusion distance across the interface has been fitted in the range of 20 to 30  $\mu\text{m}$ . Finally, a 1030 nm laser output with an output power of 4.5 W with a slope efficiency of 41.3% has been achieved pumped with 940 nm laser diode. This study has provided useful insights into developing various types of gradient rare earth doped laser ceramics for high-power laser applications.

**Keywords:** Yb: YAG; Laser ceramics; 3D printing; Gradient-doped; Active mixing

## 1. Introduction

With the increasing demand for material functionality, it is challenging for materials with a single structure to meet specific functional requirements. Additive manufacturing (AM) technology is not limited by traditional molding and machining, but has the ability to fabricate complex structures [1-3]. Specifically, it can deposit materials in specific areas to achieve the integration of designing and manufacturing. In recent years, AM technology has developed rapidly in ceramic area [4-6]. Direct ink writing (DIW), as one of AM technologies, relies on the ink extrusion from the nozzle and the linkage of a three-axis motion platform to achieve the fabrication of parts, which is convenient to develop simple structure ceramics with complex concentration profile [7].

As the ideal solid-state laser gain media, Yb: YAG( $\text{Y}_3\text{Al}_5\text{O}_{12}$ ) transparent laser ceramics has the high quantum efficiency and broad absorption and emission band, making it a selection for high-power applications [8]. The uniformly doped laser ceramics could cause thermal lens effects during the laser oscillation, leading to significant reduction of the laser beam quality [9]. It is one of the major problems to overcome for practical application of high power lasers. Gradient-doped laser ceramics with proper gain profiles can effectively alleviate the thermal distribution inside the gain media, demonstrating the very attractive potentials for solving this technical challenge [10, 11].

Generally, gradient-doped laser ceramics fabrication methods mainly include dry pressing, tape casting and bonding technology [12-15]. Li et al. [11] designed a five-segment Nd: YAG laser ceramics slab with dual concentrations, and achieved a 7.08 kW power laser output. Ter-Gabrielyan et al. [16] first reported a graded Er: YAG rod using tape casting, and a slope efficiency of 56.9% at 1645 nm has been demonstrated. Besides, complex-configuration laser crystals are also used for high-energy laser output [17, 18]. Although gradient-doped laser ceramics have shown great potentials for high-power laser applications, their difficult fabrication process is one of the biggest challenges, and thus limits the further development of such ceramics. Although dry pressing is simple, it is difficult to accurately control the layer thickness of different components in gradient-doped ceramics. For tape casting, it is necessary to fabricate raw tape with different components, which greatly increases the difficulty of forming. Moreover, the more complex the structure is, the more difficult the forming is. And the more complex the structure is, the more difficult the forming is. Ideally for laser gain media, it should be designable, and it can give the biggest advantages for laser engineers to design the solid-state lasers to meet demanding applications.

DIW opens a new way for gradient-doped laser ceramics. In recent years, some scholars have explored multi-material DIW systems with a chamber design, by which the mixing homogeneity and accuracy of the slurries

have been studied to achieve a well printing effect [19-22]. DIW with active mixing can fabricate multi-component graded structures, and only two slurries must be prepared. Also, the fabrication difficulty does not increase with the number of gradient components. The feed ratios of the slurries can be controlled to customize the matching between the designed and the actual processes. Seeley et al. [23] printed dual-component YAG laser rods by DIW with a chamber which a smoother interface refractive index fluctuation has been achieved, and optical distortion has been reduced. Moreover, various types of YAG laser ceramics by the DIW method have been reported including Nd: YAG ceramic laser rod with top-hat doping profile, Yb: YAG ceramic with longitudinal graded doping and Yb: YAG thin disk with radially graded doping [24]. However, the details of the fabrication process are not systematically introduced and only some simple graded samples are displayed. Although DIW via active mixing has the advantages of design flexibility in the gradient-doped laser ceramics preparation, there has been little research on the process complexity and controllability.

In this work, a facile approach to fabricate gradient-doped Yb: YAG laser ceramics by DIW with a home-made active mixing module using only two slurries has been proposed. The process parameters including the rotating speed and the switching delay volume between different components of the mixing module have been investigated to explore the influences on performances of preparing gradient-doped green bodies. The proposed method enabling the gradient-doped 0-5-10-5-0 at. % Yb: YAG laser ceramics fabrication has been successfully demonstrated. Then, the microstructure, optical property and ions diffusion behavior of the laser ceramics have been characterized. Finally, the gradient-doped laser ceramic has been processed to verify the laser performance.

## **2. Materials and methods**

### ***2.1. Ceramic slurries preparation***

The preparation process of 0 and 10 at. % Yb: YAG water-based slurries has been shown in Fig. 1(a). The commercial  $\text{Al}_2\text{O}_3$  (99.99 wt. % purity, Taimei Chemical Co., Ltd., Japan),  $\text{Y}_2\text{O}_3$  (99.99 wt. % purity, Jiahua Advanced Material Resources Co., Ltd., Jiangyin, China) and  $\text{Yb}_2\text{O}_3$  (99.99 wt. % purity, Rare-Chem. Hi-Tech. Co., Ltd., Huizhou, China) powders have been stoichiometrically weighed according to the formula of  $\text{Y}_3\text{Al}_5\text{O}_{12}$  and  $(\text{Y}_{0.9}\text{Yb}_{0.1})_3\text{Al}_5\text{O}_{12}$ . Then, the powders, deionized water and 0.6 wt. % dispersant (Dolapix CE-64, Zschimmer & Schwarz, Germany) have been mixed under the 50 vol. % solid loading, and ball milled at 250 rpm for 1 h to produce low viscosity slurries, which have been further adjusted by adding 0.5 wt. % hydroxyethyl cellulose (HEC, Shanghai Macklin Biochemical Co., Ltd., China) in terms of the printability. The final slurries have been well mixed and degassed in a planetary vacuum mixer at 1000 rpm for 30 s, followed by 2000 rpm for 30 s. The details about the preparation of slurries have been provided in our previous work[25]. The rheology behaviors of the slurries have been shown in Fig. 2. In Fig. 2(a), it can be seen that the viscosity of the slurry decreases with the increase of the shear rate, exhibiting shear thinning effect. This indicates that the slurry can smoothly flow out of the nozzle when under pressure. Fig. 2(b) shows the moduli of the slurry as a function of the shear stress. When the shear stress is low, the storage modulus ( $G'$ ) greater than the loss modulus ( $G''$ ) indicates that the slurry is in a solid-like state. As the shear stress

increases, when the loss modulus is greater than the storage modulus, indicating that the slurry is in liquid-like state. This solid-liquid transition characteristic is a basic requirement for the slurry in direct ink writing.

**2.2. Fabrication method of ceramic parts**

The fabrication devices shown in Fig. 1(b) includes an active mixing module and a three-axis motion platform. The mixing module mainly comprises a feed unit and a mixing chamber. The feed unit includes two mutually independent dual-channel syringe pumps and two metal syringes. The screws drive the syringe pumps, and the feed of the screw determines the slurry volume. The mixing chamber consists of two inlets, one outlet and one plain rotation shaft. The diameter of the mixing shaft is 3 mm, the inner diameter of the mixing chamber is 3.5 mm, the gap on one side is 0.25 mm, and the length of the mixing area is 20 mm. The present feed syringes are directly linked to the feed inlets to minimize the influence of frictional resistance along the pipes, since when the feed unit connects the mixing chamber through curved or long pipes, it will not only cause a waste of slurries in the pipes but also affect the feed accuracy due to the deformation of the pipes in the actual printing process. Also, the outlet connected with a printing needle can be adjusted according to the resolution requirements. Finally, a U-shaped seal and a flexible gasket seal the mixing module. The rotation shaft is connected with the drive motor through the coupling, and the drive motor provides power to control the shaft rotation speed to ensure the mixing homogeneity of the slurries.

The printing path has been programmed through the open-source slicing software Cura, which can generate G-code files containing path information. Fig. 1(c) shows the mixing chamber and the path programming. In the printing process, gradient structure green bodies have been realized by changing the feed ratios of the two slurries, and they are fabricated through mutual coordination and cooperation between the three-axis motion platform and mixing module to execute the path files at the same time. Printed green body and post-processing ceramic has been provided in Fig. 1(d).

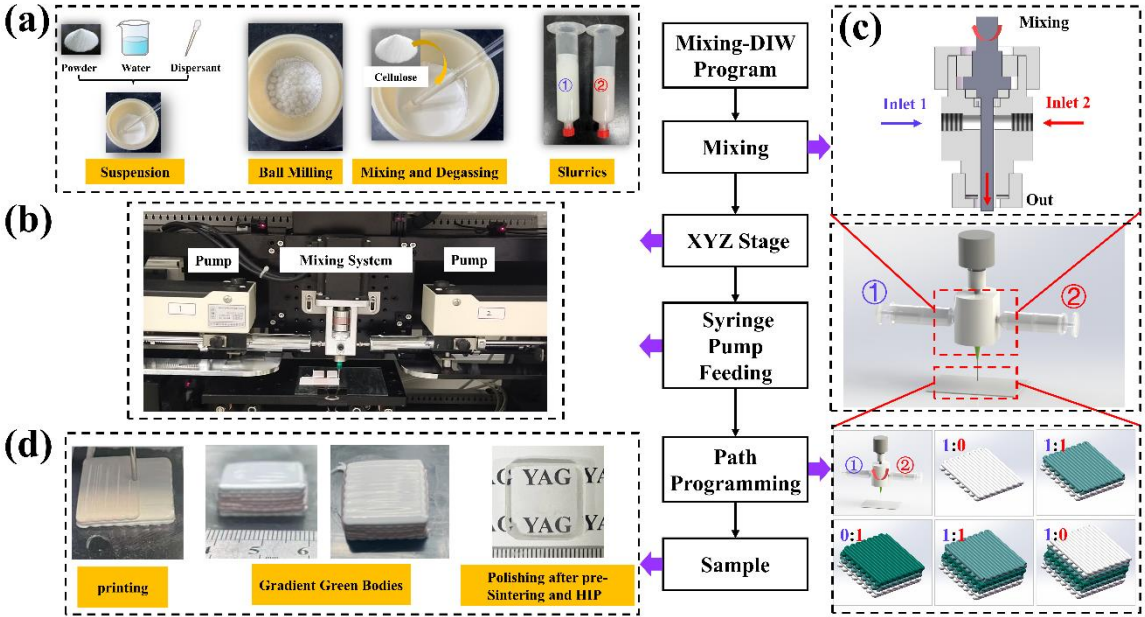


**Fig. 1.** Experimental process. (a) The preparation of slurries; (b) DIW device with active mixing; (c) The mixing chamber and path programming; (d) Green body and the sintered Yb: YAG laser ceramics.

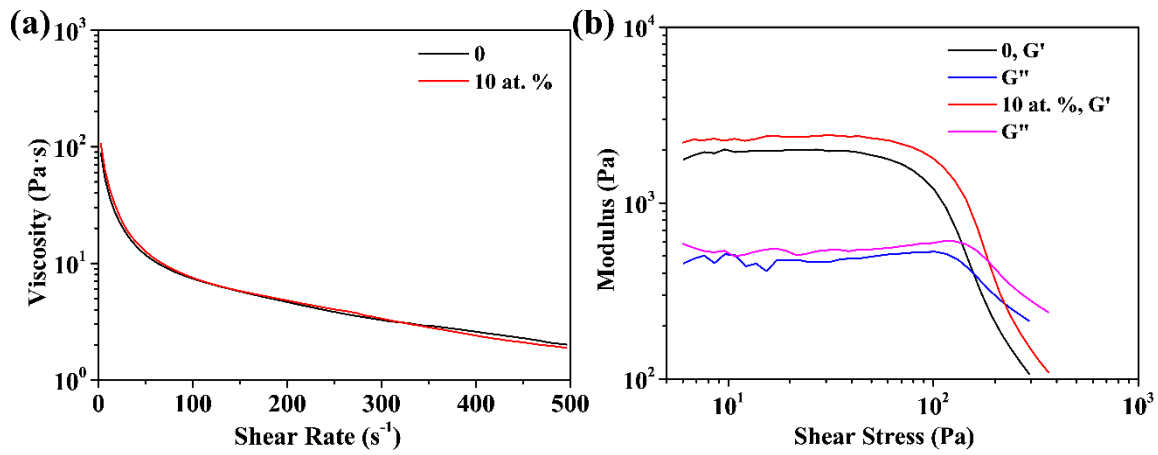


Fig. 2. Rheology behaviors of the slurries. (a) Viscosity and (b) Amplitude sweeping curves.

### 2.3. Characterization

The rheological properties of the slurries have been characterized by a rotational rheometer (Haake Viscotester iQ Air, Thermo Electron GmbH, Germany). A flat plate with a diameter of 20 mm has been selected, and the constant temperature (25 °C) of the test platform has been controlled. The homogeneity of mixtures under different rotating speeds, the distances of mixing delay and the elements' distribution at the printing interfaces have been determined by energy dispersive spectrometer (EDS, FEI Magellan 400, FEI, USA). The fracture surface morphology of the green bodies has been observed using the scanning electron microscope (SEM, FEI Magellan 400, FEI, USA). Furthermore, the in-line transmittance of the polished ceramics has been measured by an ultraviolet-visible spectrophotometer (V-770, JASCO Corporation, Japan). To observe the Yb ions concentration profile across the interface of the gradient-doped laser ceramics, the laser ablation-inductively coupled plasma-mass spectrometry including a quadrupole-based X Series II ICP-MS system (Thermo Fisher, USA) and an NWR-213 laser ablation system (NewWave, USA) has been used in this experimental test.

## 3. Results and discussion

### 3.1. Mixing homogeneity

The mixing homogeneity of the slurries during printing is fundamental, directly affecting the performance of the laser ceramics. A too low rotating speed will lead to uneven mixing, and a too high rotating speed will cause heating in the mixing chamber, which is not friendly to the water-based slurries, and thus influence the rheology behaviors of the mixed slurries. Therefore, it is particularly important to control the rotation speed in a reasonable range.

The degree of mixing of the slurries at different rotating speeds has been observed at the feed rate of 0.1 mL/min of each inlet. The mixing schematic diagram can be seen in Fig. 1(c), when the proportion of mixture is greatly different, it requires a higher speed to achieve the homogeneity of the mixture. Fig. 3 shows the Yb element surface distribution diagram at the section of extrusion filaments. It can be seen that the distribution of Yb element presents 'yin' and 'yang' with clear boundary at 0 rpm, and the mixing homogeneity gradually improves greater from 0 to 200 rpm, and keeps consistently at 200 rpm and above by EDS mapping results. Finally, 300 rpm has been chosen as the experimental parameter to ensure the homogeneity of the slurries

under different feed ratios.

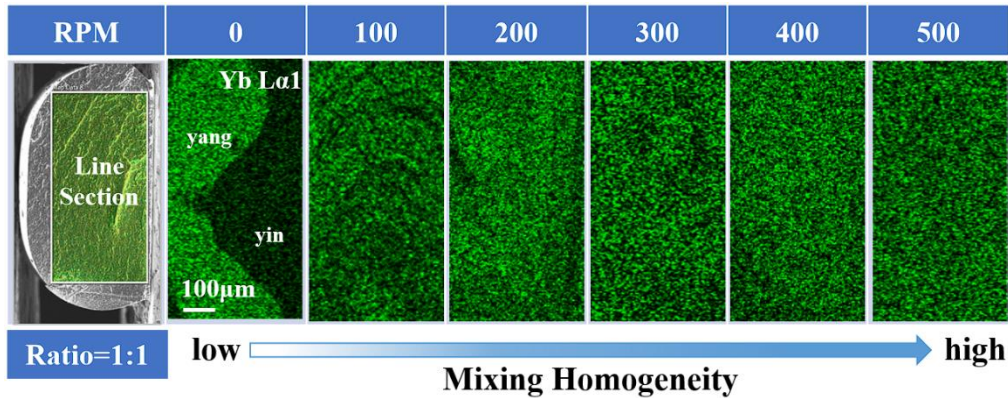


Fig. 3. EDS of Yb distribution at different rotating speeds.

### 3.2. Extrusion delays

Under the circumstances of a specific total volume flow of slurries, the switch between different components can be realized by changing the volume flow of the two slurries. The material switching command acts on the feed inlets, and the response position is in the printing head, so there must be a certain delay during component switching. The delay is observed by adding a color indicator in the slurry, and the result is shown in Fig. 4.

At the early stage, the extrusion line will keep as the previous component, and the line length delay is defined as delivery delay, about 75 mm long. It corresponds to 0.0625 mL in this set-up. During the middle of the transition, the components gradually change from the former to the latter. This delay is called transition delay, which is about 195 mm long, corresponding to 0.1625 mL, and the total delay is 0.2250 mL. At last, the components are wholly transformed into the latter. The relationship between the component and the delay distance has been plotted in Fig. 4. During the actual printing process, the desired component distribution can be achieved through path programming by moving the nozzle out for discharging waste and back into the sample at specific printing points for transition delay disposal process. The concentration distribution in the ceramics can be consistent with the design curve as much as possible through reasonable use of the delivery delay and appropriate disposal of the transition delay.

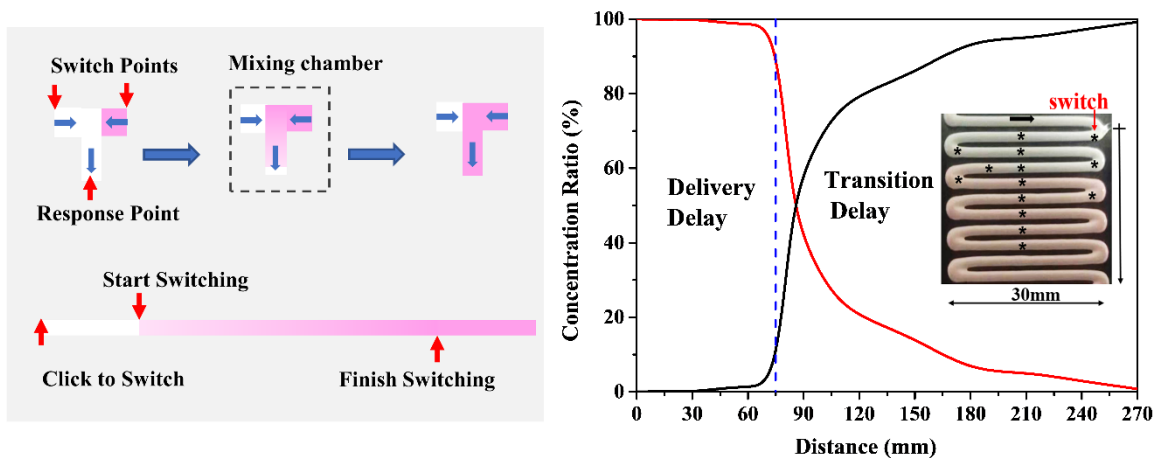


Fig. 4. Calibration of extrusion delay between different components.

### 3.3 Characterization of the ceramics

The Z-direction three-component five-stage (0-5-10-5-0 at. % Yb: YAG, each 2 layers/total 10 layers) sized

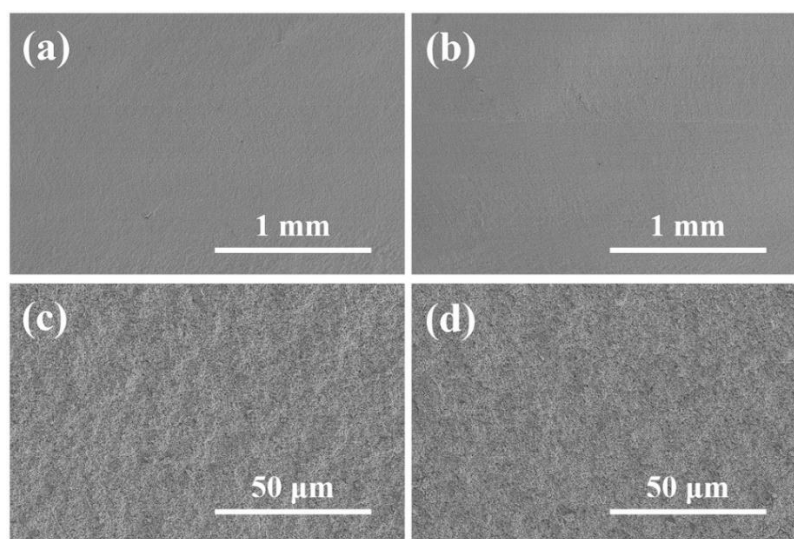
20 mm×20 mm×8 mm gradient-doped green bodies have been designed and fabricated. The printing of gradient-doped laser ceramic has been realized by switching the mixing ratios from 0:1, 1:1, 1:0, 1:1 to 0:1 when the total volume flow rate is constant. The switching delay of the slurries has been eliminated by extruding excess waste through path design. The printing nozzle with an inner diameter of 0.84 mm has been chosen in this experiment. Based on the characteristics of the material extrusion and stacking, the printing accuracy of the green bodies mainly depends on the line space and layer thickness. The optimized fabrication parameters during the printing process have been shown in Table 1.

Table 1 Optimized fabrication parameters during the printing process.

XYZ Moving Speed	Total Feed Rate of Syringe Pump	Line Space	Layer Thickness	Rotating speed of the shaft
4 mm/s	0.2 mL/min	1.25 mm	0.8 mm	300 rpm

During the drying process, water in the sample is gradually lost, and the particles gradually come together. The sample undergoes volume shrinkage and forms a green body. The printed green bodies have been dried in a constant-temperature-and-humidity box with the temperature of 25 °C and the humidity of 80% in order to prevent cracking of the green bodies caused by too rapid drying. The muffle furnace has been used to remove the organic compounds at 800 °C for 6 hours.

Since the green bodies are manufactured layer by layer through DIW, and switching between different components requires a disposal process, which means that the stacking of layers between components takes longer. It may leave printing marks inside the green bodies, which will affect the performance of the laser ceramics[26]. Fig. 5 shows the fracture surface microstructures of the gradient-doped green bodies. The printing layer thickness used in this experiment is 0.8 mm. Thus, there are at least two printing layers in Fig. 5(a) and (b). It can be seen that no delamination or void can be found, and the layers between different components are well combined. This is due to the suitable self-leveling property of the water-based slurries. As the extrusion line is deposited onto the printing substrate or the previous layer of the sample, the line between layers will be squeezed and stacked more closely due to the suitable setting of printing parameters during printing.



**Fig. 5.** The interfaces between different layers (a) (c) 0 and 5 at. % Yb: YAG and (b) (d) 5 and 10 at. % Yb: YAG.

The vacuum sintering furnace has been used for pre-sintering the green bodies at 1660 °C for 6 hours under a vacuum of around  $10^{-3}$  Pa, then hot isostatic pressing has been carried out at 1650 °C for 3 hours under 200 MPa argon gas pressure, and finally the oxygen vacancy has been removed by annealing at 1350 °C for 10 hours in air[25].

The concentration distribution of Yb element along with the doping concentration of the gradient laser ceramic has been observed. Figs. 6(a) and (d) show backscattered electron (BSE) images and Figs. 6(b) and (e) show the EDS mapping images at the printing interfaces between 0 and 5 at. % Yb: YAG and 5 and 10 at. % Yb: YAG. A clear distribution of different components has been seen by elements' detection. Since the different components have been stacked perpendicularly in space, there are minor ups and downs at the interface, which are quite straight in general. In addition, the atomic percentage of Yb element at different components have also been measured as shown in Figs. 6(g), (h) and (i). The spectrum 1 can be concluded that no Yb element has been detected. At spectrum 2 and spectrum 3, the atomic contents of Yb element are 0.7% and 1.41%, respectively, which is basically consistent with what have been designed. Figs. 6(c) and (f) show the microstructures at the printing interfaces between 0 and 5 at. % Yb: YAG and 5 and 10 at. % Yb: YAG. At a more microscopic scale, no obvious boundaries are observed between different components, and there are no pores inside the grain or on the grain boundaries, indicating the suitable sintering process parameters. And the average grain sizes at the interfaces between the different components are basically uniform. No abnormally large grains can be observed. In addition, it also can be observed that the effect of Yb ions doping on the growth of grain sizes are not significant.

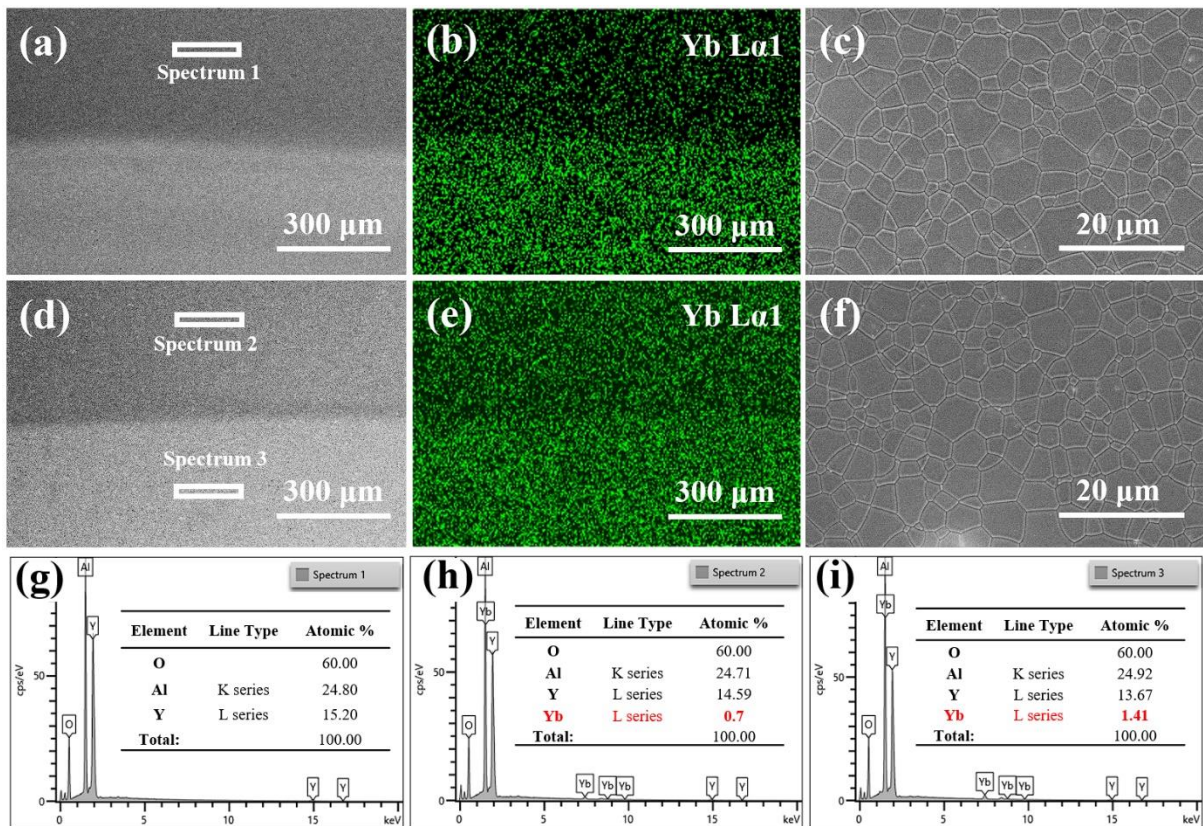


**Fig. 6.** The BSE, EDS and SEM microstructures images. (a-c) 0 and 5 at. % Yb: YAG, (d-f) 5 and 10 at. % Yb: YAG at the printing interfaces, and (g-i) EDS spectra of 0, 5, and 10 at. % Yb: YAG.

After sintering, the sample has been double-sided polished to square shape with the size of 17 mm×17 mm.

Fig. 7(a) shows the in-line transmittance curve of gradient-doped Yb: YAG laser ceramic, which reaches 82.1% at 1100 nm wavelength (4.6 mm thickness, along with the doping concentration gradient). It can be seen that the in-line transmittance of the printed gradient-doped laser ceramic decreases dramatically between 900 nm and 1100 nm, which is caused by the absorption of Yb. The absorption peak is located at approximately 940 nm. The sintering process will drive Yb ions to diffuse from high concentration to low concentration, and the diffusion behavior conforms to the Fick's second law [27]. For gradient-doped laser ceramics (0-5-10-5-0 at. % Yb: YAG), Yb ions will diffuse during sintering. Fig. 7(b) shows the concentration distribution of Yb element along the section measured by laser ablation-inductively coupled plasma-mass spectrometry and the fitting curves of the concentration distribution of Yb, which can be fitted according to Eq. (1)[28].

$$c(x) \propto I(x) = I_0 \operatorname{erfc}[\alpha(x-x_0)] \quad (1)$$

The relationship between Yb concentration  $c$  and mass spectrum signal strength  $I$  is linear. And the average diffusion distance  $\langle x \rangle$  can be calculated by Eq. (2).

$$\langle x \rangle = 1/\alpha\sqrt{\pi} \quad (2)$$

It can be seen that there are three Yb doping concentration stages, which represent 0, 5, and 10 at. % Yb: YAG, respectively. The signal strength also shows that the concentration of Yb element is consistent with the designed profile, and it also reflects that there is a good mixing homogeneity of the slurries. The average diffusion distance of the gradient-doped laser ceramics is in the range of 20 to 30  $\mu\text{m}$  by fitting the obtained data according to Eq. (2), which have similar diffusion distances with traditional ceramic preparation methods[29].

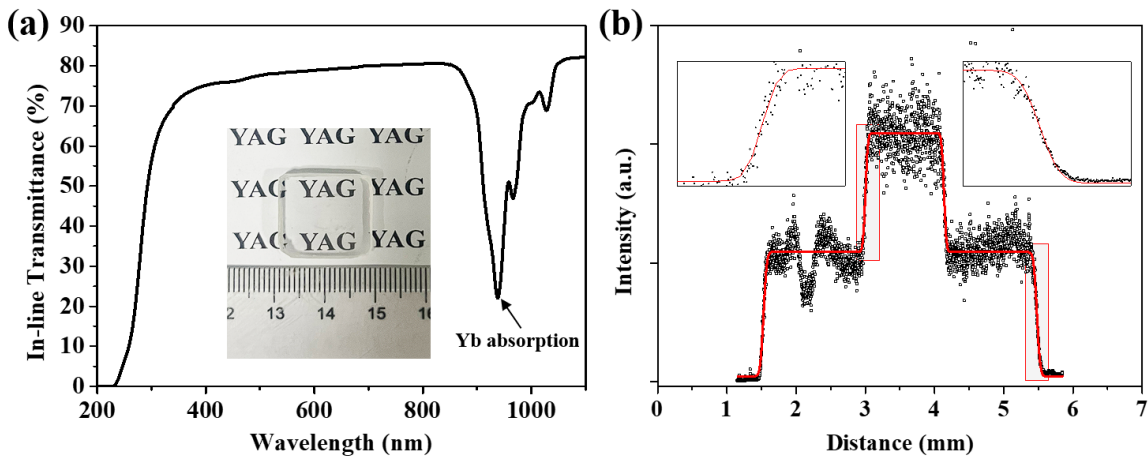


**Fig. 7.** Gradient-doped laser ceramic of (a) In-line transmittance curves of 4.6 mm thickness (insert:

double-sided polished ceramic sample); (b) The concentration distribution of Yb element between layers.

The laser experiments are performed with LD end pump, and the pumping source is a 940 nm fiber-coupled diode laser with a core diameter of 105  $\mu\text{m}$ . The resonant cavity is plane-parallel resonator [30]. The output coupling mirror with the transmissions of 15% have been conducted to verify the laser output performance of gradient 0-5-10-5-0 at. % Yb: YAG with dimensions of 3 mm $\times$ 3 mm $\times$ 4.6 mm, as shown in Fig. 8. Under the same pumping conditions, the laser output power increases with the increase of the absorbed pump power. With the absorbed pump power of 16.1 W at the output coupling mirror transmission of 15%, a laser output of 4.5 W has been obtained at 1030 nm with a slope efficiency of 41.3%. In addition, the laser properties of different fabrication methods have been compared, as shown in Table 2. It can be seen that the slope efficiency

of laser ceramics prepared by direct ink writing in this experiment is comparable to that of traditional fabrication methods. The laser properties in this work are in the leading position compared to other additive manufacturing results.

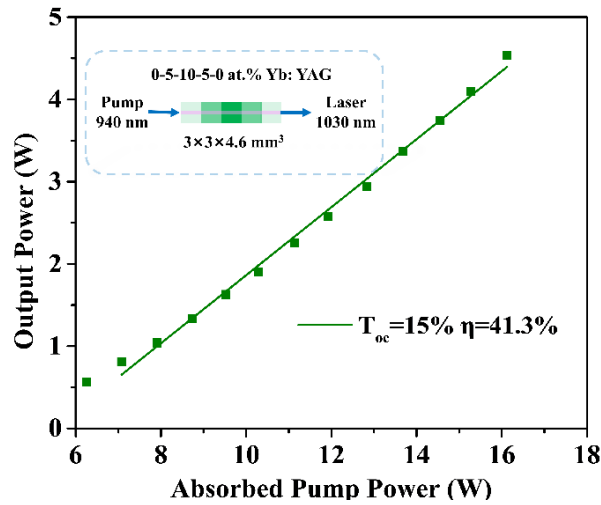


Fig. 8. Output power vs absorbed pump power of 0-5-10-5-0 at. % Yb: YAG laser ceramic.

Table 2 The ceramic laser properties of different fabrication methods.

Fabrication methods	Structures	Components	Slope efficiency	Ref.
Direct ink writing	Gradient-doped	0-5-10-5-0 at. % Yb: YAG	41.3%	This work
Direct ink writing	Top-hat	YAG/ 2 at. % Nd Gradient	~15.0%	[23]
Stereolithography	Uniform	10 at. % Yb: YAG	17.6%	[31]
Tape casting	Gradient-doped	0-0.6-1.5-0.6-0 at. % Yb: YAG	45.0%	[32]
Dry pressing	Slab	YAG/1.0 at. % Nd: YAG/YAG	10.1%	[33]

DIW with active mixing can fabricate different shapes according to the design requirements, and it can also give full play to the greatest advantage of additive manufacturing in the fabrication of gradient continuous laser ceramics than traditional preparation methods.

#### 4. Conclusion

Gradient-doped Yb: YAG laser ceramics have been successfully fabricated by a facile approach, which depends on DIW with a home-made active mixing module using only two slurries. The major printing parameters such as rotating speed and switching delay volume between different components of the mixing module have been experimentally tested and optimized for the different type of printing path, to obtain uniform and accurate element distribution of gradient-doped laser ceramics.

Based on these optimized process parameters, the multi-component (0-5-10-5-0 at. % Yb: YAG) green bodies have been manufactured by executing the path files and changing the feed ratios of YAG and 10 at. % Yb: YAG in appropriate positions. The interfaces between different components of green body and ceramic have been characterized. Highly transparent five-segment gradient-doped Yb: YAG ceramics with in-line transmittance of 82.1% at 1100 nm has been obtained successfully. Besides, the concentration distribution of Yb ions has been measured and the average diffusion distance across the interface has been fitted in the range

of 20 to 30  $\mu\text{m}$ . Finally, the 940 nm laser diode has been used as the pumping source to achieve the gradient-doped Yb: YAG laser ceramic with 1030 nm laser output of 4.5 W with a slope efficiency of 41.3%.

In conclusion, the proposed approach can fabricate gradient-doped laser ceramics and also sheds lights on the possibility of manufacturing more complex gradient-doped laser ceramics for future high powder laser applications.

## Declaration of competing interest

The authors declare that they have no known competing financial interests or personal relationships that could have appeared to influence the work reported in this paper.

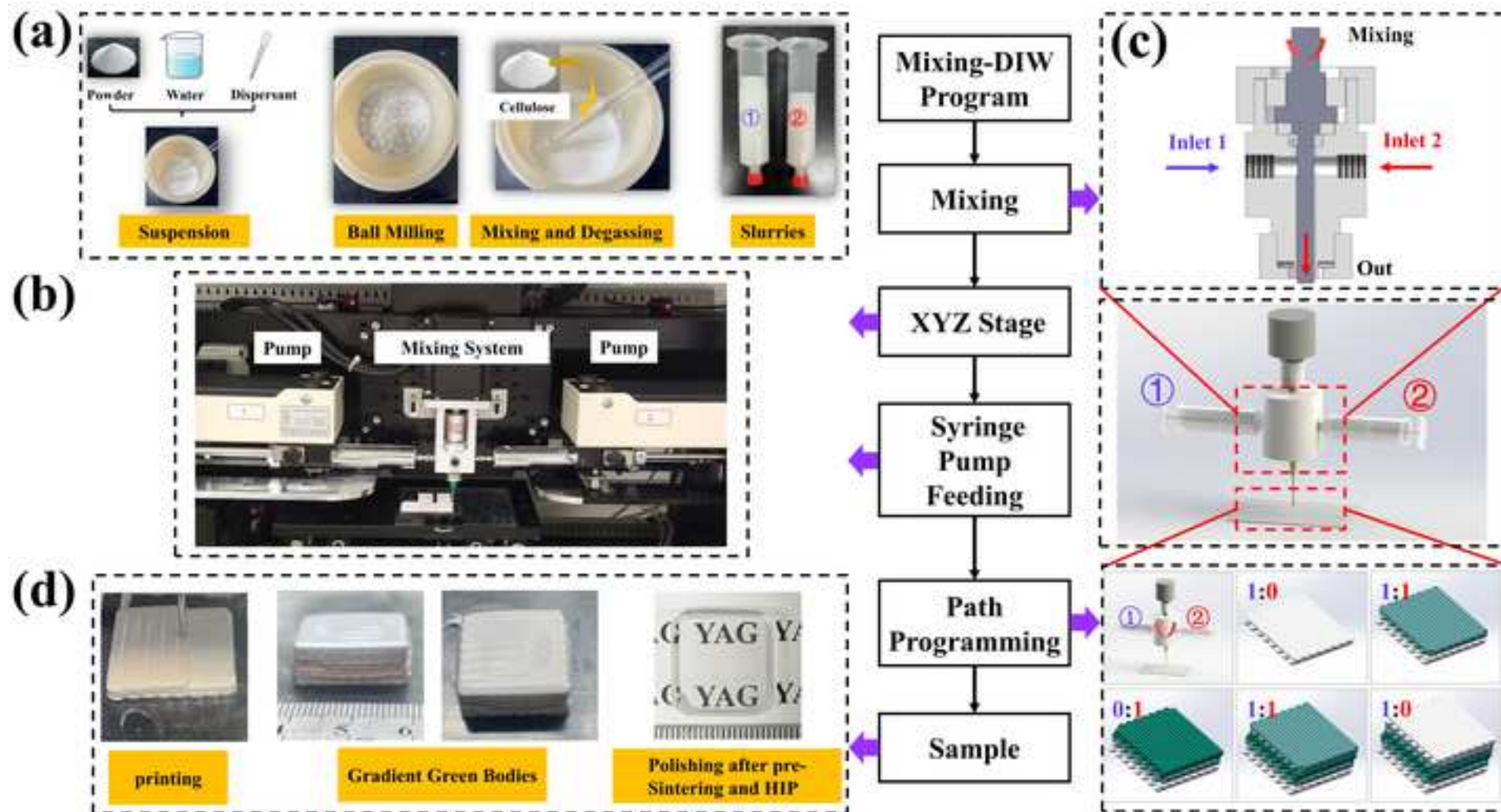
## Acknowledgements

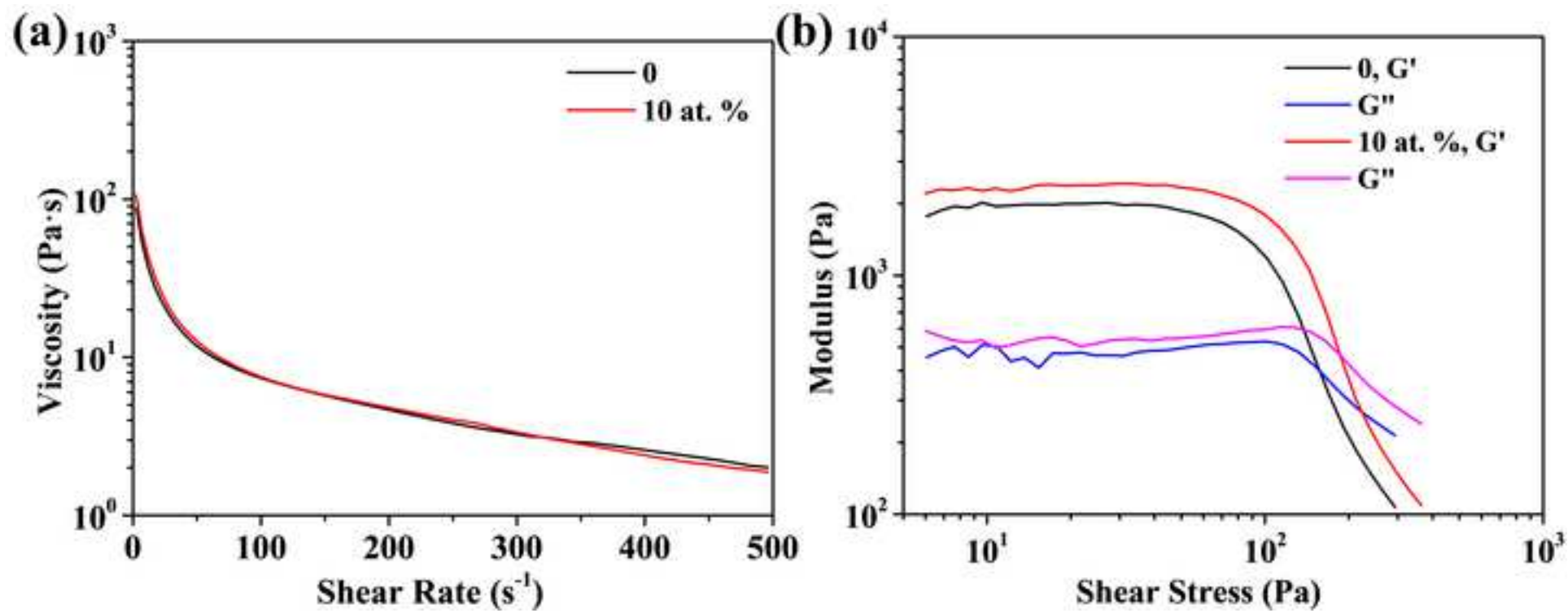
This work was supported by Jiangsu Provincial Key Research and Development Program (Grant No. BE2022069-2), National Natural Science Foundation of China (Grant No. 52130207) and National Basic Science Research Program of China (Grant No. JCKY2021203B032).

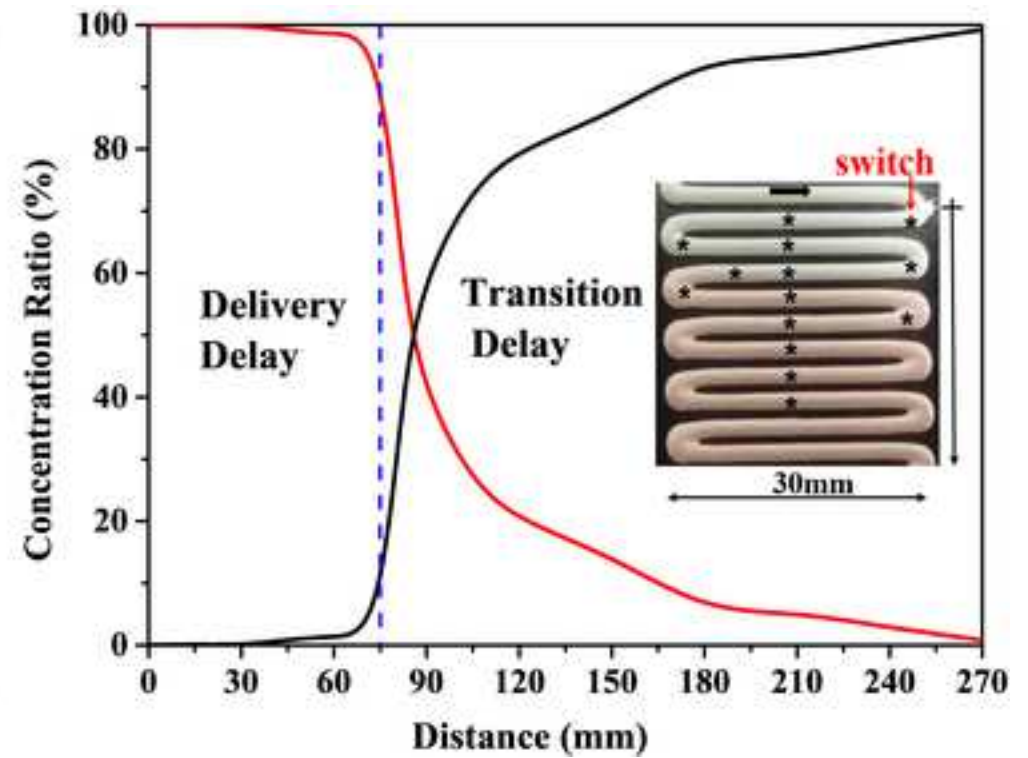
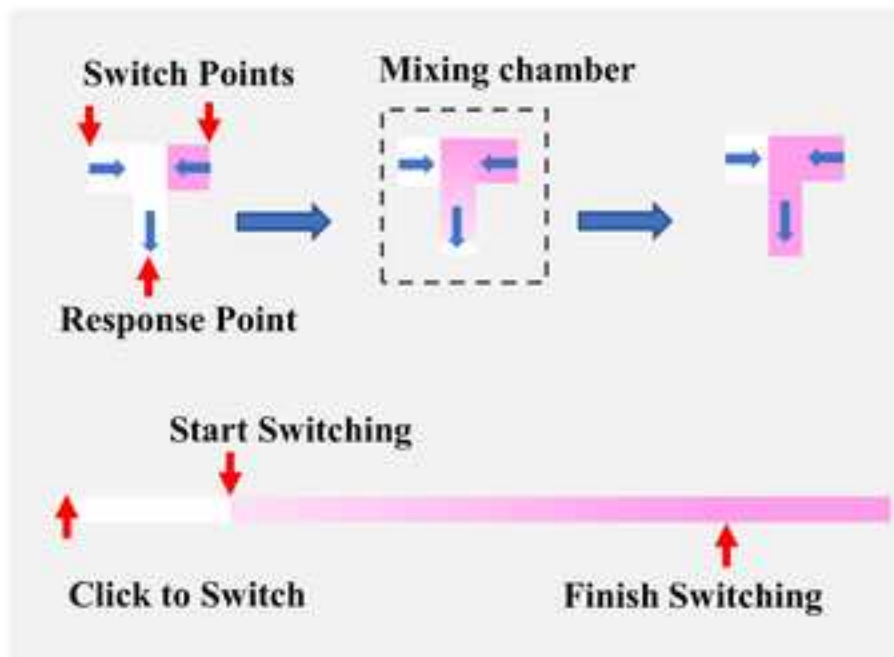
## References

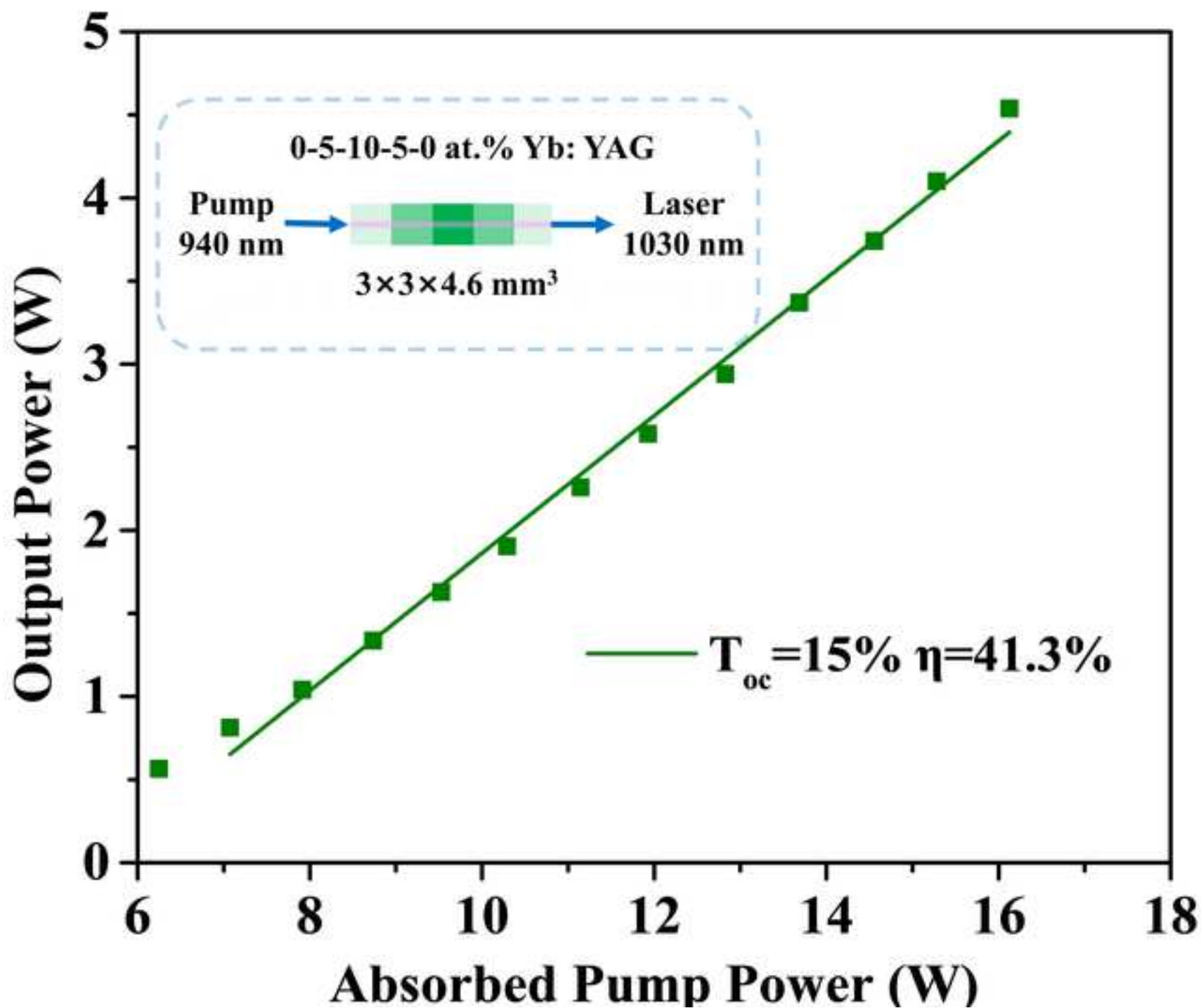
- [1] Li Y, Feng Z Y, Hao L, et al. A review on functionally graded materials and structures via additive manufacturing: from multi-scale design to versatile functional properties. *Adv Mater Technol* 2020; 5(6): 1900981.
- [2] Rocha V G, Saiz E, Tirichenko I S, et al. Direct ink writing advances in multi-material structures for a sustainable future. *J Mater Chem A* 2020; 8(31): 15646-15657.
- [3] Rafiee M, Farahani R D, Therriault D. Multi-material 3D and 4D printing: A survey. *Adv Sci* 2020; 7(12): 1902307.
- [4] Zhang D W, Peng E, Borayek R, et al. Controllable ceramic green-body configuration for complex ceramic architectures with fine features. *Adv Funct Mater* 2019; 29(12): 1807082.
- [5] Shahzad A, Lazoglu I. Direct ink writing (DIW) of structural and functional ceramics: Recent achievements and future challenges. *Compos Part B: Eng* 2021; 225: 109249.
- [6] Li W, Armani A, Martin A, et al. Extrusion-based additive manufacturing of functionally graded ceramics. *J Eur Ceram Soc* 2021; 41(3): 2049-2057.
- [7] Lewis J A. Colloidal processing of ceramics. *J Am Ceram Soc* 2004; 83(10): 2341-2359.
- [8] Ikesue A, Aung Y L. Ceramic laser/solid-state laser. *Process of Ceramic* 2021; pp. 33-72.
- [9] Ikesue A, Aung Y L. Ceramic laser materials. *Nat Photonics* 2008; 2(12): 721-727.
- [10] Dong J Y, Cui J W, Wen Y, et al. High-effective mitigation of thermal effect in multi segment and multi concentration (MSMC) Tm: YAG crystal. *Infrared Phys Technol* 2022; 122: 104104.
- [11] Li M, Hu H, Gao Q S, et al. A 7.08-kW YAG/Nd: YAG/YAG composite ceramic slab laser with dual concentration doping. *IEEE Photonics J* 2017; 9(4): 1-10.
- [12] Fujioka K, Sugiyama A, Fujimoto Y, et al. Ion diffusion at the bonding interface of undoped YAG/Yb:YAG composite ceramics. *Opt Mater* 2015; 46: 542-547.
- [13] Ma C, Tang F, Zhu J, et al. Cation diffusion at the interface of composite YAG/Re: LuAG (Re = Nd or Yb) transparent ceramics. *J Eur Ceram Soc* 2016; 36(10): 2555-2564.
- [14] Tang F, Cao Y, Huang J, et al. Multilayer YAG/Re:YAG/YAG laser ceramic prepared by tape casting and vacuum sintering method. *J Eur Ceram Soc* 2012; 32(16): 3995-4002.

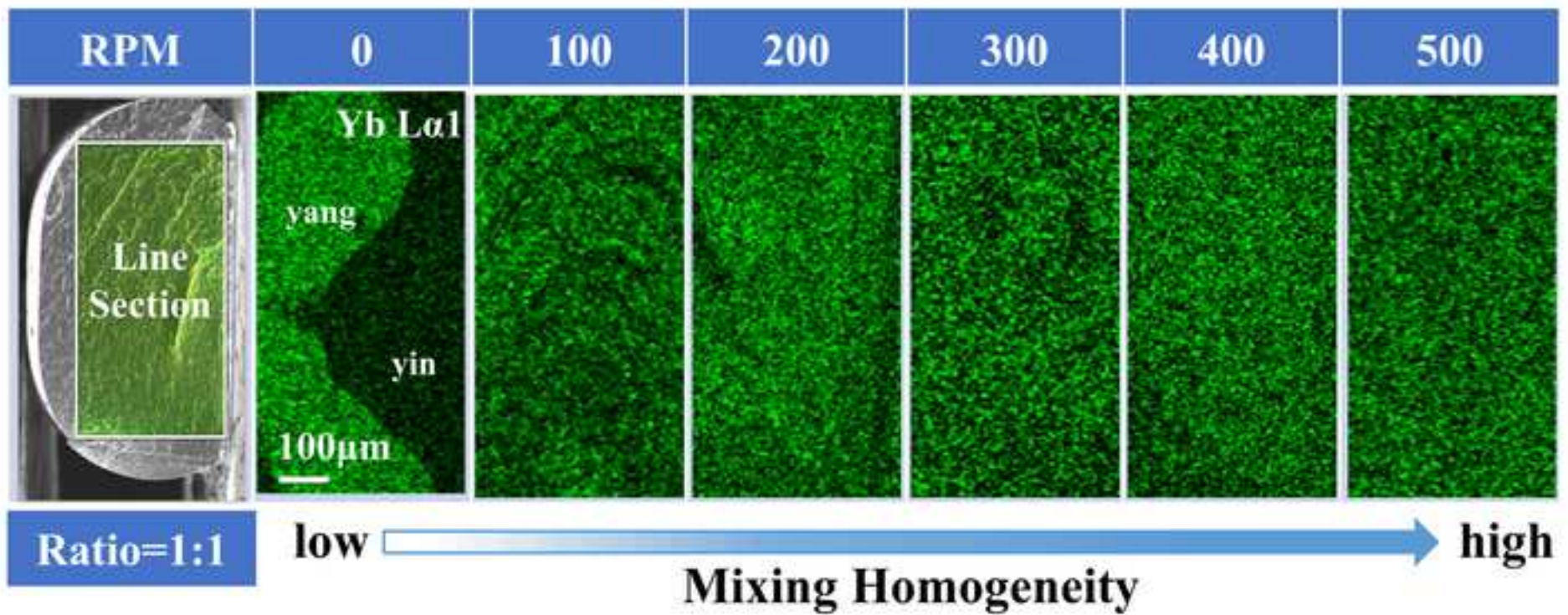
- [15] Ikesue A, Aung Y L, Kamimura T, et al. Composite laser ceramics by advanced bonding technology. *materials* (Basel) 2018; 11(2): 271.
- [16] Ter-Gabrielyan N, Merkle L D, Kupp E R, et al. Efficient resonantly pumped tape cast composite ceramic Er:YAG laser at 1645 nm. *Opt Lett* 2010; 35(7): 922-924.
- [17] De Vido M, Meissner D, Meissner S, et al. Characterisation of adhesive-free bonded crystalline Yb:YAG for high energy laser applications. *Opt Mater Express* 2017; 7(2): 425-432.
- [18] Wei M E, Cheng T Q, Dou R Q, et al. High-peak-power electro-optically Q-switched laser with a gradient-doped Nd:YAG crystal. *Opt Lett* 2021; 46(19): 5016-5018.
- [19] Ortega J M, Golobic M, Sain J D, et al. Active mixing of disparate inks for multimaterial 3D printing. *Adv. Mater. Technol* 2019; 4(7): 1800717.
- [20] Ober T J, Foresti D, Lewis J A. Active mixing of complex fluids at the microscale. *Proc Natl Acad Sci* 2015; 112(40): 12293-12298.
- [21] Pelz J S, Ku N, Shoulders W T, et al. Multi-material additive manufacturing of functionally graded carbide ceramics via active, in-line mixing. *Addit Manuf* 2021; 37: 101647.
- [22] Golobic A M, Durban M D, Fisher S E, et al. Active mixing of reactive materials for 3D printing. *Adv Eng Mater* 2019; 21(8): 1900147.
- [23] Seeley Z, Yee T, Cherepy N, et al. 3D printed transparent ceramic YAG laser rods: Matching the core-clad refractive index. *Opt Mater* 2020; 107: 110121.
- [24] Seeley Z M, Rudzik T J, Phillips I R, et al. Additive manufacturing of transparent ceramic laser gain media - rods, thin disks, and planar waveguides, in *Laser Congress 2020*, Optica Publishing Group, Washington, D.C., 2020, p. AW1A.1.
- [25] Ji H H, Zhao J, Chen J, et al. A novel experimental approach to quantitatively evaluate the printability of inks in 3D printing using two criteria. *Addit Manuf* 2022; 55: 102846.
- [26] Ji H H, Zhao J, Chen J, et al. Direct ink writing of cellulose-plasticized aqueous ceramic slurry for YAG transparent ceramics. *Mrs Commun* 2022; 12(2): 206-212.
- [27] Crank J. *The Mathematics Of Diffusion*, second ed., Clarendon Press, Oxford, 1956.
- [28] Yagi H. The physical properties of composite YAG ceramics. *Laser Phys Lett* 2005; 15(9): 1338-1344.
- [29] Rudzik T J, Seeley Z M, Ryerson F J, et al. Counter-ion effect on the diffusion behavior of Yb, Lu, and Nd ions in YAG transparent ceramics. *Opt Mater: X* 2022; 13: 100132.
- [30] Wang L, Huang H, Shen D, et al. Highly stable self-pulsed operation of an Er:Lu<sub>2</sub>O<sub>3</sub> ceramic laser at 2.7μm. *Laser Phys Lett* 2017; 14(4): 045803.
- [31] Hostasa J, Schwentenwein M, Toci G, et al. Transparent laser ceramics by stereolithography. *Scr Mater* 2020; 187(1): 194-196.
- [32] Tian F, Jiang N, Liu Y, et al. Fabrication and properties of multistage gradient doping Yb:YAG laser ceramics. *J Eur Ceram Soc* 2022; 106(4): 2309-2316.
- [33] Liu W, Zeng Y, Li J, et al. Sintering and laser behavior of composite YAG/Nd:YAG/YAG transparent ceramics. *J Alloys Compd* 2012; 527: 66-70.

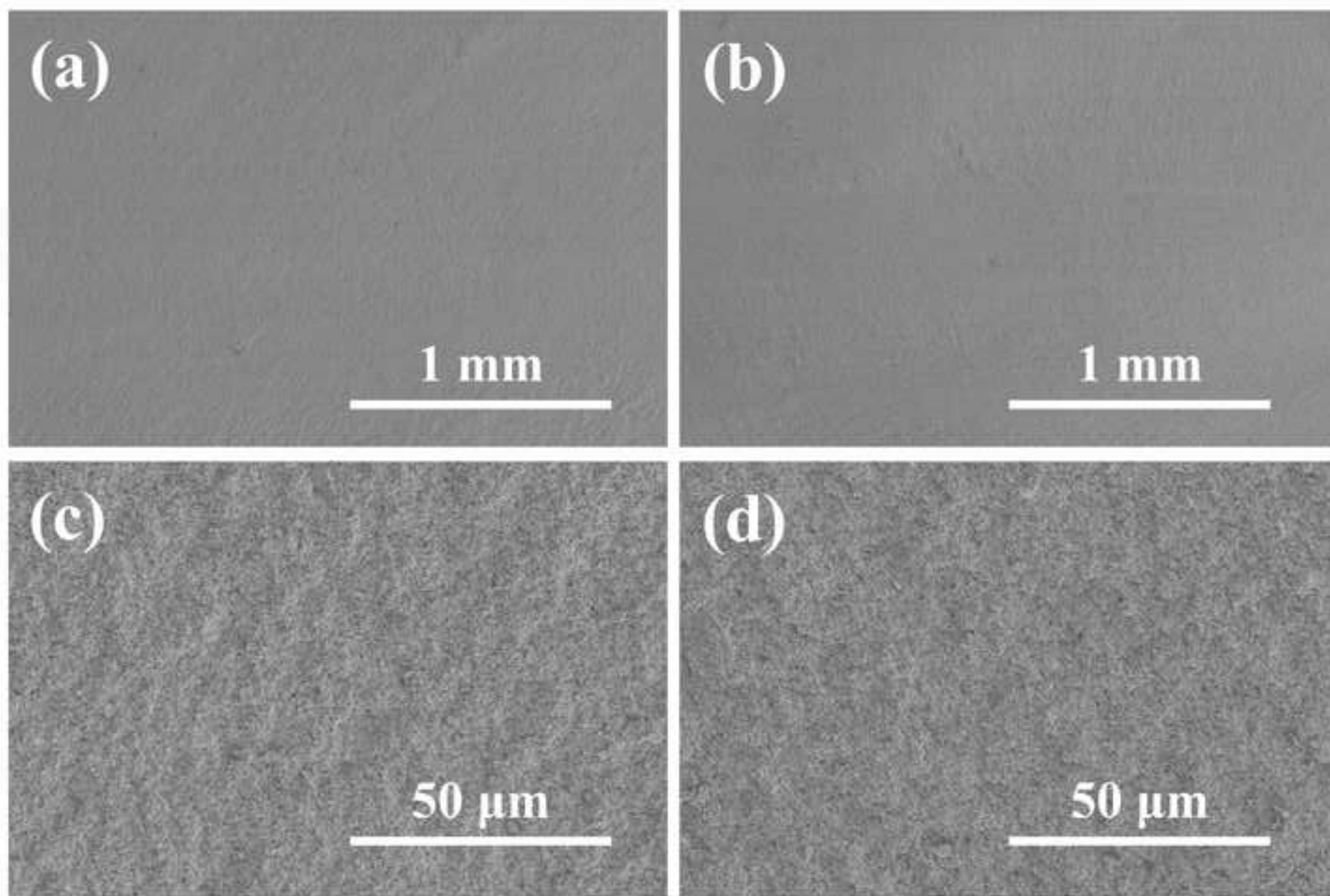


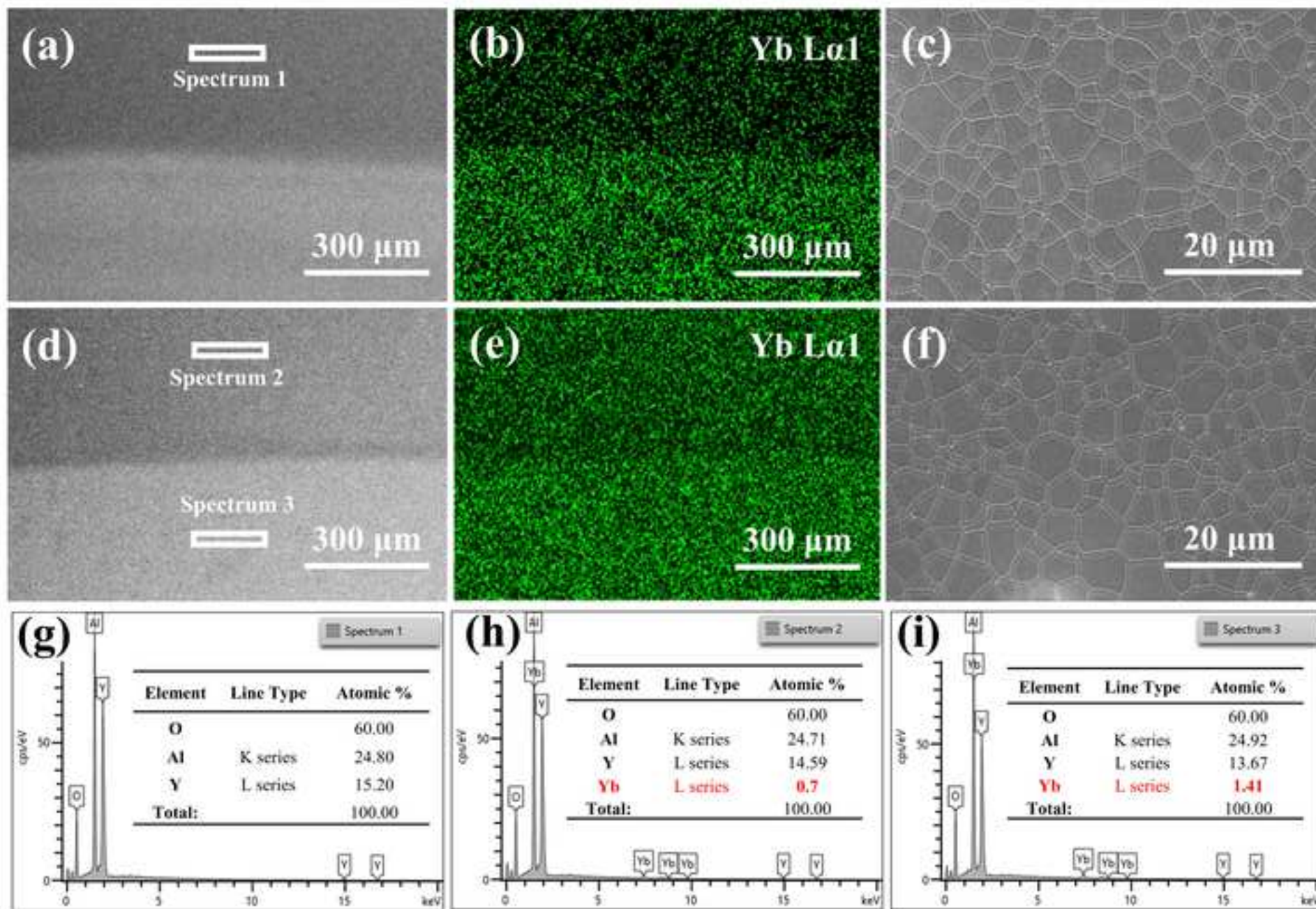


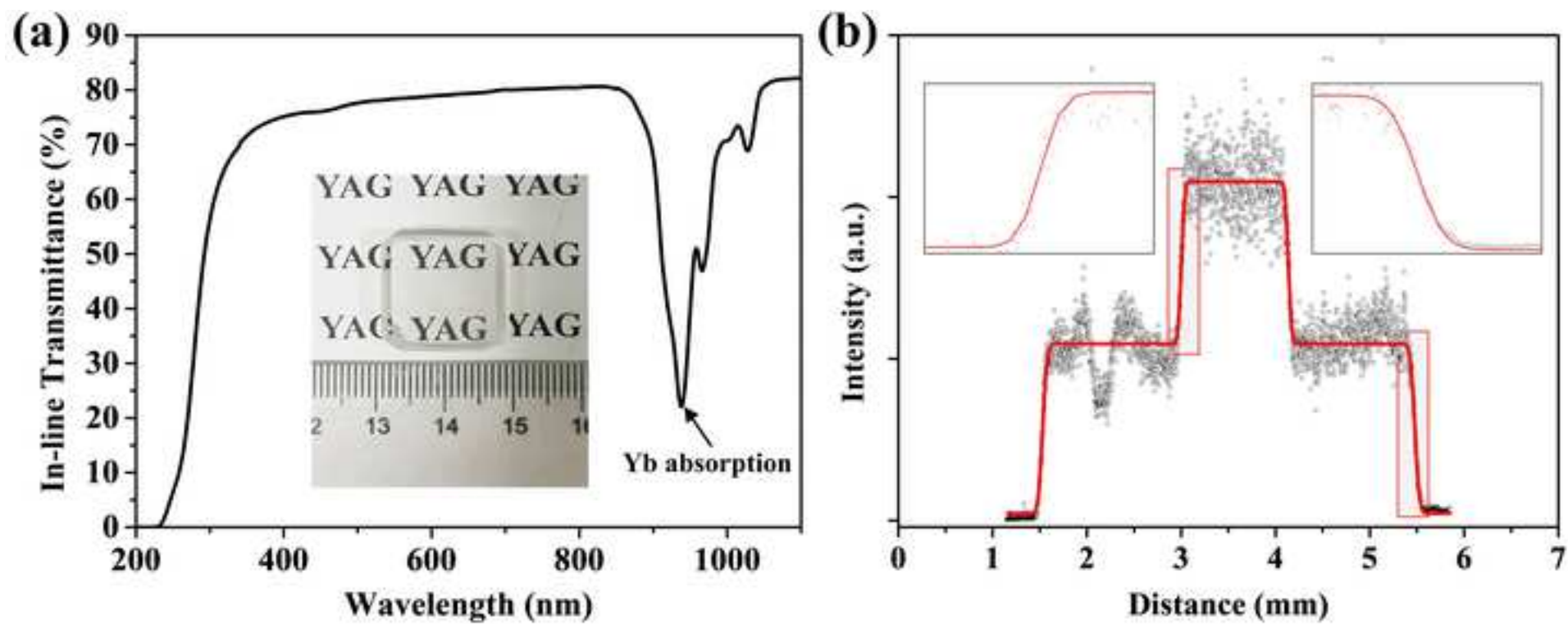












## **Highlights**

- Gradient-doped Yb: YAG green bodies have been fabricated by active mixing 3D printing
- Highly transparent gradient-doped Yb: YAG laser ceramic with 82.1% in-line transmittance at 1100 nm has been obtained
- A 1030 nm laser output with an output power of 4.5W with a slope efficiency of 41.3% has been achieved pumped with 940 nm laser diode